

RATE-DEPENDENT NONLOCAL CRYSTAL PLASTICITY: IMPLEMENTATION AND BOUNDARY LAYERS

Eduardo Bittencourt^a and Alan Needleman^b

^a*Escola de Engenharia, Universidade Federal do Rio Grande do Sul, Av. Osvaldo Aranha, 99, Porto Alegre, RS 90035-190, Brazil, eduardo.bittencourt@ufrgs.br*

^b*Division of Engineering, Brown University, Providence, RI 02912, USA, needle@brown.edu.**

Keywords: Crystal plasticity, size-dependence, finite elements, boundary layers, rate sensitivity.

Abstract. A finite element implementation of a rate-dependent version of the nonlocal crystal plasticity theory of Gurtin (J Mech Phys Solids 50:5-32 (2002)) is presented. The algorithm used is equivalent to a conventional forward gradient method when the nonlocal terms are absent. Attention is restricted to small deformations so that geometry changes are neglected. A two dimensional analysis of simple shear of a constrained single crystal strip with two symmetric slip systems is carried out. The results are compared with results of the corresponding rate-independent theory. Boundary layers develop that give rise to size effects. For the rate sensitivity in the calculations here, it is found that the boundary layers are not as strongly dependent on the dissipative hardening as in the rate-independent case. In cases without dissipative hardening, the rate-dependent results essentially coincide with those of the rate-independent theory for large characteristic lengths. However, for small characteristic lengths, rate effects can substantially change the boundary layers.

*Currently visiting at the Department of Materials Science and Engineering, University of North Texas, Denton, TX, 76203, USA

1 INTRODUCTION

Consideration of the effects of material rate sensitivity in single crystals has been analyzed numerically for instance in Pierce et al. (1983) and Asaro and Needleman (1985). Consideration of such effects permits also that certain combinations of strain hardening and crystal geometries, which can not be analyzed by rate-independent formulations, be studied. Also, rate-dependent formulations eliminate ambiguities in determining active slip systems, since all slip systems with a non-zero resolved shear stress contribute to the plastic deformation.

These studies were restricted to classical crystal plasticity theories. However, classical plasticity predicts a size independent response, which is in disagreement with experiments when gradients of plastic flow occur (see for instance Ebeling and Ashby, 1966, Brown and Ham, 1971, Fleck et al. 1994, etc.). One source of size effects arises from the presence of geometrically necessary dislocations (Nye, 1953, Ashby, 1970). To take into account this effect, phenomenological nonlocal plasticity theories have been proposed as in Fleck and Hutchinson (1993, 1997, 2001), Acharya and Bassani (2000), etc. Here, we are specifically focus on the nonlocal theory of Gurtin (2002). In a previous study, Bittencourt et al. (2003), it was found that a rate-independent implementation of Gurtin's (2002) theory gave a good representation of results of discrete dislocation plasticity calculations.

Numerical implementations of nonlocal plasticity theories using rate-dependent constitutive laws can be found, for instance, in Borg et al (2006). However this work focuses on isotropic plasticity. In the present paper, we present an algorithm to deal with nonlocal rate-dependent crystal plasticity. The theory follows the work of Gurtin (2002) and the numerical implementation of rate sensitivity follows the work of Pierce et al. (1983).

The boundary value problem considered is simple shear of a constrained layer (Shu et al., 2001). In this problem, a local plasticity theory would predict a uniform shear strain in the layer. Discrete dislocation plasticity and various nonlocal plasticity theories give rise to a very different behavior: the shear strain in the layer is not uniform, and boundary layers evolve with increasing deformation.

We begin by outlining the nonlocal plasticity theory proposed in Gurtin (2002), restricted to infinitesimal deformations and rate-dependent material behavior. Two sources of hardening are accounted for in this theory; dissipative hardening associated with an increase in slip resistance and energetic hardening associated with an increase in free energy due to a density of geometrically necessary dislocations. The discretization of the nonlocal theory within a finite element framework and the implicit time integration procedure are then described. Results for simple shear of a constrained layer obtained using the present rate dependent implementation are compare with results of the rate independent theory in Bittencourt et al. (2003).

2 FORMULATION

The present formulation is based on nonlocal crystal plasticity theory due to Gurtin (2002). We restrict attention to small deformations and the material is considered rate-dependent.

The gradient of the displacement vector, u_i , is decomposed as the sum of an elastic and a plastic part. The plastic part occurs by crystallographic slip on a set of slip planes. With $s_i^{(\beta)}$ and $m_i^{(\beta)}$ unit vectors specifying the slip direction and the slip plane normal, respectively, for slip system β , the plastic part of the displacement gradient is given by

$$u_{ij}^p = \sum_{\beta} \gamma^{(\beta)} s_i^{(\beta)} m_j^{(\beta)} \quad (1)$$

with $\gamma^{(\beta)}$ the total slip on the system β . (We use Greek superscripts, without the summation convention, to label the slip systems.)

The balance laws are derived from the principle of virtual work, in which fields $\pi^{(\beta)}$ and $\xi_i^{(\beta)}$ work-conjugate to slips and slip gradients are introduced:

$$\int_B \left[T_{ij} \delta u_{i,j} + \sum_{\beta} (\pi^{(\beta)} - \tau^{(\beta)}) \delta \gamma^{(\beta)} + \sum_{\beta} \xi_i^{(\beta)} \delta \gamma_{,i}^{(\beta)} \right] dV = \int_{\partial B_q} \sum_{\beta} q^{(\beta)} \delta \gamma^{(\beta)} dA + \int_{\partial B_t} t_i \delta u_i dA \quad (2)$$

Here T_{ij} is the standard (Cauchy) stress tensor with $T_{ij} = T_{ji}$. Since eq. (2) must hold for variations δu and $\delta \gamma^{(\beta)}$, we have the classical balance

$$T_{ij,j} = 0 \quad (3)$$

and a microforce balance

$$\pi^{(\alpha)} - \tau^{(\alpha)} - \xi_{i,i}^{(\alpha)} = 0 \quad (4)$$

Here $\tau^{(\alpha)}$ are resolved stresses and can be calculated as

$$\tau^{(\alpha)} = P_{ij}^{(\alpha)} T_{ij} \quad , \quad P_{ij}^{(\alpha)} = \frac{1}{2} \left(s_i^{(\alpha)} m_j^{(\alpha)} + s_j^{(\alpha)} m_i^{(\alpha)} \right) \quad (5)$$

where $\pi^{(\alpha)}$ is the flow resistance.

We consider power law rate sensitivity and write $\pi^{(\alpha)}$ as:

$$\pi^{(\alpha)} = \sigma^{(\alpha)} f(\dot{\gamma}^{(\alpha)}) = \sigma^{(\alpha)} \frac{\dot{\gamma}^{(\alpha)}}{\dot{a}^{(\alpha)}} \left| \frac{\dot{\gamma}^{(\alpha)}}{\dot{a}^{(\alpha)}} \right|^{m-1} \quad (6)$$

Finally, $\xi_i^{(\alpha)}$ is termed a microstress and it is related to the net Burgers vector (or the density of geometrically necessary dislocations). In the calculations here it has the form (Gurtin, 2002):

$$\xi_i^{(\alpha)} = \ell^2 \pi^{(\alpha)} s_i^{(\alpha)} \sum_{\beta} s_j^{(\alpha)} s_j^{(\beta)} \gamma_{,k}^{(\beta)} s_k^{(\beta)} \quad (7)$$

where ℓ is a characteristic length. In the absence of microstresses, we have a standard local theory, as can be seen replacing eq. (6) in eq. (4).

The quantity $\sigma^{(\alpha)}$ is the slip resistance and is written in the rate form as:

$$\dot{\sigma}^{(\alpha)} = \sum_{\beta} h_{\alpha\beta} |\dot{\gamma}^{(\beta)}| \quad (8)$$

The form of the hardening modulus $h_{\alpha\beta}$ matrix used here follows Pierce et al. (1983),

$$h_{\alpha\beta} = qH + (1 - q)H\delta_{\alpha\beta} \quad (9)$$

where q is the ratio of latent hardening to self hardening (typically taken to be in the range 1 – 1.4).

Boundary conditions in which either

$$t_i = \sigma_{ij} n_j \quad \text{or} \quad u_i \quad (10)$$

and either

$$q^{(\beta)} = \xi_i^{(\beta)} n_i \quad \text{or} \quad \gamma^{(\beta)} \quad (11)$$

are prescribed at each point of the boundary. Subsequently, a boundary condition of the form $\gamma^{(\beta)} = 0$ is referred to as a micro-clamped boundary condition and a boundary condition of the form $q^{(\beta)} = 0$ is termed a micro-free boundary condition. Microscopic boundary conditions were studied in details in Gurtin and Needleman (2004) and it was shown that the micro-clamped boundary condition as defined above can be too restrictive in some cases.

3 FINITE ELEMENT IMPLEMENTATION

The finite element method is used as spatial discretization of the domain. Independent discretizations of the displacement field $u_i(x_1, x_2)$ and the slip field $\gamma^{(\beta)}(x_1, x_2)$ are used. In each finite element, these fields are related to nodal values according to

$$\gamma^{(\beta)}(x_1, x_2) = \sum_{N=1}^{NN} \phi^N(x_1, x_2) \Gamma^{N,(\beta)} \quad (12)$$

$$u_i(x_1, x_2) = \sum_{N=1}^{NN} \phi^N(x_1, x_2) U_i^N \quad (13)$$

where NN is the number of nodes per finite element, and U_i^N and $\Gamma^{N,(\beta)}$ are the nodal values of displacement and slip, respectively. Thus, the number of unknowns per node is two plus the number of slip systems. Eight node isoparametric quadratic elements with serendipity interpolation functions ϕ^N are used for both u_i and $\gamma^{(\beta)}$. As a consequence, u_i and $\gamma^{(\beta)}$ are continuous across element boundaries, but the derivatives $u_{i,j}$ and $\gamma_{,i}^{(\beta)}$ are not. Within each element, the integration in eq. (2) is carried out using 3×3 integration points.

For a representative node N of finite element e and time $t + \Delta t$, we calculate

$$F_i^N = \int_{Be} T_{ij,(t+\Delta t)} \phi_{,j}^N dv - \int_{\partial Be_t} t_{i,(t+\Delta t)} \phi^N da \quad (14)$$

$$M^{N,(\beta)} = \int_{Be} \left\{ \left(\tau_{(t+\Delta t)}^{(\beta)} - \pi_{(t+\Delta t)}^{(\beta)} \right) \phi^N - \xi_{i,(t+\Delta t)}^{(\beta)} \phi_{,i}^N \right\} dv + \int_{\partial Be_q} q_{(t+\Delta t)}^{(\beta)} \phi^N da \quad (15)$$

with the surface integrals appearing only if one or more sides of the element are on a surface where t_i or $q^{(\beta)}$ is prescribed. With the assembled vectors from eq. (14) and eq. (15) denoted by \mathbf{F} and \mathbf{M} , respectively, nodal equilibrium at time $t + \Delta t$ requires that

$$\mathbf{F} = \mathbf{0} \quad , \quad \mathbf{M} = \mathbf{0} \quad (16)$$

4 SOLUTION PROCEDURE

An incremental-iterative strain-driven algorithm is used. It is assumed that the configuration at time t is in equilibrium and an equilibrium solution at time $t + \Delta t$ is sought. It is assumed that the configuration $(U_i, \Gamma^{(\alpha)})$ at time t and $t + \Delta t$ are known. Current increment of slips $(\Delta \gamma^{(\alpha)})$ are associated to rate of slips by:

$$\Delta \gamma^{(\alpha)} = \dot{\gamma}_{(t+\Delta t)}^{(\alpha)} \Delta t \quad (17)$$

4.1 Integration of Stresses

In small-deformations, increments of the Cauchy stresses ΔT_{ij} can be calculated as¹:

$$\Delta T_{ij} = L_{ijkl} \left(\Delta \epsilon_{kl} - \sum_{\beta} P_{kl}^{(\beta)} \Delta \gamma^{(\beta)} \right) \quad (18)$$

$\Delta \gamma^{(\beta)}$ is the increment in slips, and is obtained from the finite element nodal values as

$$\Delta \gamma^{(\beta)} = \sum_{N=1}^{NN} \phi^N \Delta \Gamma^{N,(\beta)} \quad (19)$$

$\Delta \epsilon_{ij}$ is the increment in total strains, that can be calculated as

$$\Delta \epsilon_{ij} = \frac{1}{2} (\Delta u_{i,j} + \Delta u_{j,i}) \quad (20)$$

the gradients $\Delta u_{i,j}$ are calculated as for a conventional size independent solid. Then,

$$\Delta u_{i,k} = \sum_{N=1}^{NN} \phi_{,k}^N \Delta U_i^N \quad (21)$$

L_{ijkl} is the Hooke tensor

$$L_{ijkl} = K \delta_{ij} \delta_{kl} + 2G (\delta_{ik} \delta_{jl} - \frac{1}{3} \delta_{ij} \delta_{kl}) \quad (22)$$

K is the incompressibility modulus, G the shear modulus. The updated value of the stress tensor is then:

$$T_{ij,(t+\Delta t)} = T_{ij,(t)} + \Delta T_{ij} \quad (23)$$

Resolved stresses are updated according to eq. (5). The flow resistance can be also updated (see eq. (8)) as

$$\sigma_{(t+\Delta t)}^{(\alpha)} = \sigma_{(t)}^{(\alpha)} + \sum_{\beta} h_{\alpha\beta} |\Delta \gamma^{(\beta)}| \quad (24)$$

Increments of microstresses $\xi_i^{(\alpha)}$ are calculated according equation eq. (7) as

$$\Delta \xi_i^{(\alpha)} = \ell^2 \pi^{(\alpha)} s_i^{(\alpha)} \sum_{\beta} s_j^{(\alpha)} s_j^{(\beta)} \Delta \gamma_{,k}^{(\beta)} s_k^{(\beta)} \quad (25)$$

Updated microstress is then,

$$\xi_{i,(t+\Delta t)}^{(\alpha)} = \xi_{i,(t)}^{(\alpha)} + \Delta \xi_i^{(\alpha)} \quad (26)$$

¹In the first iteration of each time-step, when $\Delta \gamma^{(\alpha)}$ is considered equal to the previous time-step value ($\dot{\gamma}_{(t)}^{(\alpha)} \Delta t$), a better approximation of Cauchy stresses can be obtained by eq. (47) (see Section 4.2),

$$\Delta T_{ij} = L_{ijkl}^{tan} \Delta \epsilon_{kl} - \sum_{\alpha} \sum_{\beta} R_{ij}^{(\alpha)} M_{\alpha\beta} \dot{\gamma}_{(t)}^{(\beta)} \Delta t$$

In eq. (25), the gradient of slips $\Delta\gamma_{,k}^{(\beta)}$ comes from nodal values of slip $\Delta\Gamma^{(\beta)}$, as follows:

$$\Delta\gamma_{,k}^{(\beta)} = \sum_{N=1}^{NN} \phi_{,k}^N \Delta\Gamma^{N,(\beta)} \quad (27)$$

Because for a rate-dependent solid all points undergo visco-plastic flow, the stress update procedure is performed for all points of the body. By way of contrast, the strong form (eq. (4)) used for a rate-independent solid to decide whether a node is plastic or elastic (Bittencourt et al. (2003)) is not used.

4.2 Forward Gradient Method

In this section an application of a forward gradient method to visco-plastic constitutive equation will be described. The formulation follows that in Pierce et al. (1983) but is here restricted to small-deformations.

In order to build a tangent operator, as we will discuss later, the exponential term introduced in equation eq. (6) is linearized. This linearization can be obtained by a Taylor expansion of $\pi_{(t)}^{(\alpha)}$ as follows:

$$\pi_{(t+\Delta t)}^{(\alpha)} = \pi_{(t)}^{(\alpha)} + \left. \frac{d\pi^{(\alpha)}}{dt} \right|_{(t)} \Delta t \quad (28)$$

The above derivative can be written as:

$$\frac{d\pi^{(\alpha)}}{dt} = m\sigma^{(\alpha)} \frac{\dot{\gamma}^{(\alpha)}}{(\dot{a}^{(\alpha)})^2} \left| \frac{\dot{\gamma}^{(\alpha)}}{\dot{a}^{(\alpha)}} \right|^{m-2} \left| \frac{d\dot{\gamma}^{(\alpha)}}{dt} + \frac{\dot{\gamma}^{(\alpha)}}{\dot{a}^{(\alpha)}} \left| \frac{\dot{\gamma}^{(\alpha)}}{\dot{a}^{(\alpha)}} \right|^{m-1} \right|_{(\dot{\gamma})} \frac{d\sigma^{(\alpha)}}{dt} \quad (29)$$

Using eq. (8) and eq. (6), replacing eq. (29) in eq. (28) and identifying $\text{sgn}(\Delta\gamma^{(\beta)})$ with $\text{sgn}(\dot{\gamma}_{(t)}^{(\beta)}) = \text{sgn}(\tau^{(\beta)})$, we have:

$$\Delta\pi^{(\alpha)} = \frac{m\pi^{(\alpha)}}{\dot{\gamma}^{(\alpha)}} \left| \frac{\dot{\gamma}^{(\alpha)}}{\dot{a}^{(\alpha)}} \right|^{m-2} \Delta\dot{\gamma}^{(\alpha)} + \frac{\pi^{(\alpha)}}{\sigma^{(\alpha)}} \left| \frac{\dot{\gamma}^{(\alpha)}}{\dot{a}^{(\alpha)}} \right|^{m-1} \sum_{\beta} h_{\alpha\beta} \Delta\gamma^{(\beta)} \text{sgn}(\tau^{(\beta)}) \quad (30)$$

This expression is the same used by Borg et al. (2006) to calculate increments of flow stress. Considering that,

$$\Delta\dot{\gamma}^{(\alpha)} = \dot{\gamma}_{(t+\Delta t)}^{(\alpha)} - \dot{\gamma}_{(t)}^{(\alpha)} \quad (31)$$

and multiplying both sides of eq. (30) by Δt , this equation can be also written as:

$$\Delta\pi^{(\alpha)} = \frac{m\pi^{(\alpha)}}{\Delta\gamma^{(\alpha)}} \left| \frac{\dot{\gamma}^{(\alpha)}}{\dot{a}^{(\alpha)}} \right|^{m-2} \Delta\gamma^{(\alpha)} + m\pi^{(\alpha)} \left| \frac{\dot{\gamma}^{(\alpha)}}{\dot{a}^{(\alpha)}} \right|^{m-1} \frac{\pi^{(\alpha)}}{\sigma^{(\alpha)}} \left| \frac{\dot{\gamma}^{(\alpha)}}{\dot{a}^{(\alpha)}} \right|^{m-1} \sum_{\beta} h_{\alpha\beta} \Delta\gamma^{(\beta)} \text{sgn}(\tau^{(\beta)}) \quad (32)$$

Updated flow resistance $\pi_{t+\Delta t}^{(\alpha)}$ is then:

$$\pi_{t+\Delta t}^{(\alpha)} = \sigma^{(\alpha)} \frac{\dot{\gamma}^{(\alpha)}}{\dot{a}^{(\alpha)}} \left| \frac{\dot{\gamma}^{(\alpha)}}{\dot{a}^{(\alpha)}} \right|^{m-1} \left| \frac{\dot{\gamma}^{(\alpha)}}{\dot{a}^{(\alpha)}} \right|_{(t)}^{m-1} + \Delta\pi^{(\alpha)} \quad (33)$$

which is the expression used in the weak form (eq. (15)) and leads to a symmetric tangent matrix.

Considering the strong/incremental form of local microscopic balance, it requires that

$$\Delta\pi^{(\alpha)} - \Delta\tau^{(\alpha)} = 0 \quad (34)$$

Replacing $\Delta\pi^{(\alpha)}$ by equation (30) and isolating $\Delta\dot{\gamma}$, we have

$$\Delta\dot{\gamma}^{(\alpha)} = \frac{\dot{\gamma}^{(\alpha)}}{m\pi^{(\alpha)}} \Big|_{(t)} \Delta\tau^{(\alpha)} - \frac{\dot{\gamma}^{(\alpha)}}{m\sigma^{(\alpha)}} \Big|_{(t)} \sum_{\beta} h_{\alpha\beta} \Delta\gamma^{(\beta)} \operatorname{sgn}(\tau^{(\beta)}) \quad (35)$$

Multiplying the equation by Δt and considering that at time t equilibrium was achieved (and then $\pi^{(\alpha)} = \tau^{(\alpha)}$),

$$\Delta\gamma^{(\alpha)} = \dot{\gamma}_{(t)}^{(\alpha)} \Delta t + \frac{\dot{\gamma}^{(\alpha)} \Delta t}{m\tau^{(\alpha)}} \Big|_{(t)} \Delta\tau^{(\alpha)} - \frac{\dot{\gamma}^{(\alpha)} \Delta t}{m\sigma^{(\alpha)}} \Big|_{(t)} \sum_{\beta} h_{\alpha\beta} \Delta\gamma^{(\beta)} \operatorname{sgn}(\tau^{(\beta)}) \quad (36)$$

The expression eq. (36) is the same as obtained by the forward gradient method of Pierce et al. (1983).

With the small-deformation approximation $\Delta\tau^{(\alpha)}$ can be calculated as:

$$\Delta\tau^{(\alpha)} = R_{ij}^{(\alpha)} \left(\Delta\epsilon_{ij} - \sum_{\beta} P_{ij}^{(\beta)} \Delta\gamma^{(\beta)} \right) \quad (37)$$

where $\Delta\epsilon_{ij}$ is the variation of total strain in the time step and $R_{ij}^{(\alpha)}$ is defined as

$$R_{ij}^{(\alpha)} = L_{ijkl} P_{kl}^{(\alpha)} \quad (38)$$

Replacing eq. (37) in eq. (36), gives

$$\Delta\gamma^{(\alpha)} = \dot{\gamma}_{(t)}^{(\alpha)} \Delta t + Q_{ij}^{(\alpha)} \Delta\epsilon_{ij} - Q_{ij}^{(\alpha)} \sum_{\beta} P_{ij}^{(\beta)} \Delta\gamma^{(\beta)} - \frac{\dot{\gamma}^{(\alpha)} \Delta t}{m\sigma^{(\alpha)}} \sum_{\beta} h_{\alpha\beta} \Delta\gamma^{(\beta)} \operatorname{sgn}(\tau^{(\beta)}) \quad (39)$$

where we used

$$Q_{ij}^{(\alpha)} = \frac{\Delta\gamma_{(t)}^{(\alpha)}}{m\tau^{(\alpha)}} R_{ij}^{(\alpha)} \quad (40)$$

Equation (39) can be written in the compact form,

$$\dot{\gamma}_{(t)}^{(\alpha)} \Delta t + Q_{ij}^{(\alpha)} \Delta\epsilon_{ij} = \sum_{\beta} \Delta\gamma^{(\beta)} N_{\alpha\beta} \quad (41)$$

with

$$N_{\alpha\beta} = \delta_{\alpha\beta} + \left(\frac{\dot{\gamma}_{(t)}^{(\alpha)} \Delta t}{m} \right) \left[\frac{R_{ij}^{(\alpha)} P_{ij}^{(\beta)}}{\tau^{(\alpha)}} + \frac{h_{\alpha\beta}}{\sigma^{(\alpha)}} \operatorname{sgn}(\tau^{(\beta)}) \right] \quad (42)$$

Inverting eq. (41) leads to

$$\Delta\gamma^{(\alpha)} = f^{(\alpha)} + F_{ij}^{(\alpha)} \Delta\epsilon_{ij} \quad (43)$$

where

$$f^{(\alpha)} = \sum_{\beta} M_{\alpha\beta} \dot{\gamma}_{(t)}^{(\beta)} \Delta t \quad (44)$$

and

$$F_{ij}^{(\alpha)} = \sum_{\beta} M_{\alpha\beta} Q_{ij}^{(\beta)} \quad (45)$$

$M_{\alpha\beta}$ is the inverse of $N_{\alpha\beta}$. The variation of Cauchy stress in the time step can be now calculated as,

$$\Delta T_{ij} = L_{ijkl} \left(\Delta \epsilon_{kl} - \sum_{\alpha} P_{kl}^{(\alpha)} \Delta \gamma^{(\alpha)} \right) \quad (46)$$

and using eq. (43) in eq. (46),

$$\Delta T_{ij} = L_{ijkl}^{tan} \Delta \epsilon_{kl} - \sum_{\alpha} \sum_{\beta} R_{ij}^{(\alpha)} M_{\alpha\beta} \dot{\gamma}_{(t)}^{(\beta)} \Delta t \quad (47)$$

with

$$L_{ijkl}^{tan} = L_{ijkl} - \sum_{\alpha} R_{ij}^{(\alpha)} F_{kl}^{(\alpha)} \quad (48)$$

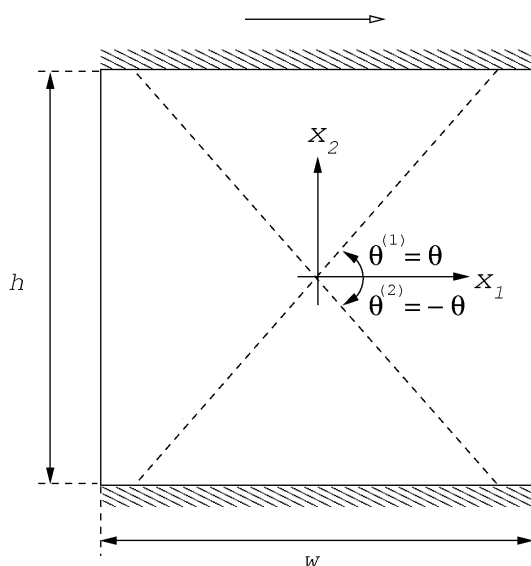


Figure 1: Simple shear of an elasto-viscoplastic layer of thickness h with two active slip system.

4.3 Iterative Scheme

In order to achieve equilibrium, an iterative Newton-Raphson scheme is used as follows:

$$\begin{pmatrix} \mathbf{K}_{UU} & \mathbf{K}_{U\Gamma} \\ \mathbf{K}_{\Gamma U} & \mathbf{K}_{\Gamma\Gamma} \end{pmatrix}_{(t+\Delta t)}^{(i-1)} \begin{Bmatrix} \Delta \mathbf{U} \\ \Delta \mathbf{\Gamma} \end{Bmatrix}_{(t+\Delta t)}^{(i)} = \begin{Bmatrix} \mathbf{F} \\ \mathbf{M} \end{Bmatrix}_{(t+\Delta t)}^{(i-1)} \quad (49)$$

where \mathbf{F} and \mathbf{M} are the assembled values of F_i^N and $M^{N,(\alpha)}$ and $\Delta \mathbf{U}$ and $\Delta \mathbf{\Gamma}$ are the assembled values of ΔU_i^N and $\Delta \Gamma^{N,(\beta)}$, respectively. The matrix in eq. (49) can be called a tangent matrix and is symmetric in the present context. The sub-matrices inside it are built from the derivatives

$$\mathbf{K}_{UU} = \left. \frac{\partial \mathbf{F}}{\partial \mathbf{U}} \right|_{(t+\Delta t)}, \quad \mathbf{K}_{U\Gamma} = \left. \frac{\partial \mathbf{F}}{\partial \mathbf{\Gamma}} \right|_{(t+\Delta t)}, \quad \mathbf{K}_{\Gamma U} = \left. \frac{\partial \mathbf{M}}{\partial \mathbf{U}} \right|_{(t+\Delta t)}, \quad \mathbf{K}_{\Gamma\Gamma} = \left. \frac{\partial \mathbf{M}}{\partial \mathbf{\Gamma}} \right|_{(t+\Delta t)}$$

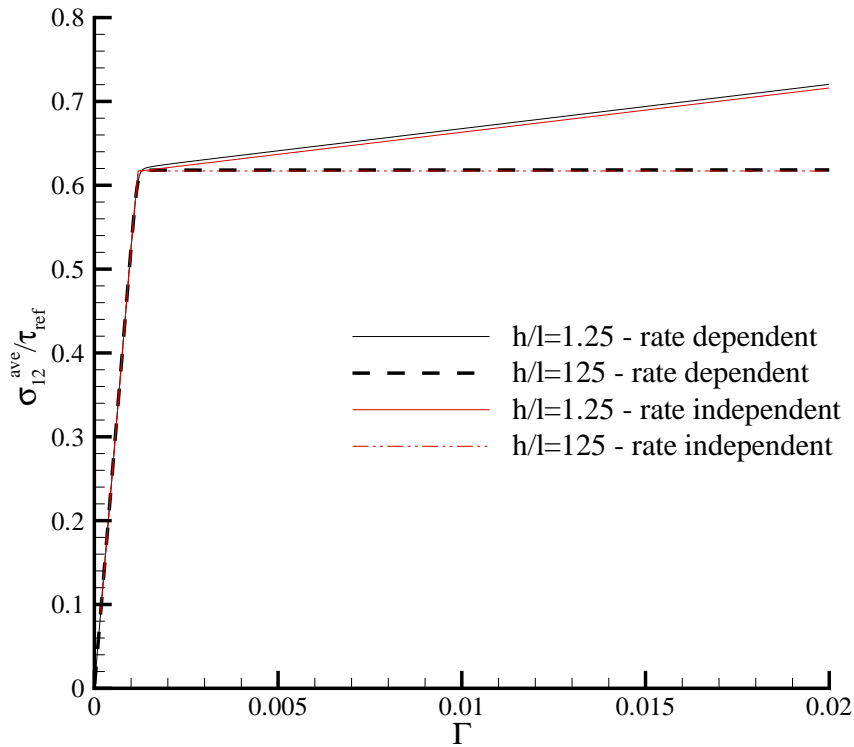


Figure 2: Shear stress-shear strain relations with $H = 0$ (no dissipative hardening), comparing the present rate-dependent results with corresponding rate-independent results (Bittencourt *et al.*, 2003).

At each iteration i , the system eq. (49) is solved, $\Delta \mathbf{U}$ and $\Delta \mathbf{\Gamma}$ are calculated and T_{ij} , $\xi_i^{(\alpha)}$, etc are updated and then \mathbf{F} and \mathbf{M} . Iterations will occur until the Euclidean norm of $\Delta \mathbf{F}$ and $\Delta \mathbf{M}$ are sufficiently small.

5 AN EXAMPLE PROBLEM

A simple shear of a crystalline constrained layer is analyzed here. This example has been analyzed using discrete dislocation plasticity in Shu *et al.* (1999) and using rate-independent crystal plasticity in Bittencourt *et al.* (2003).

A strip, of height h in the x_2 -direction, is considered, with shearing along the x_1 -direction as illustrated in Figure 1. Plane strain and quasi-static loading conditions are assumed, and the strip is unbounded in the x_1 - and x_3 -directions. The crystal is taken to have two symmetrically oriented slip systems.

The macroscopic boundary conditions are

$$\begin{aligned} u_1 = 0 \quad , \quad u_2 = 0 \quad \text{along } x_2 = 0; \\ u_1 = U(t) = h\Gamma(t) \quad , \quad u_2 = 0 \quad \text{along } x_2 = h, \end{aligned} \quad (50)$$

where $\Gamma(t)$ is the prescribed shear. In the constrained layer problem we restrict attention to monotonic loading, so that the prescribed shear rate satisfies $\dot{\Gamma} > 0$.

In addition, all field quantities are required to be periodic in x_1 with period w ; for example, $u_i(x_1, x_2) = u_i(x_1 + jw, x_2)$ for any integer j . For the local theory and for the discrete

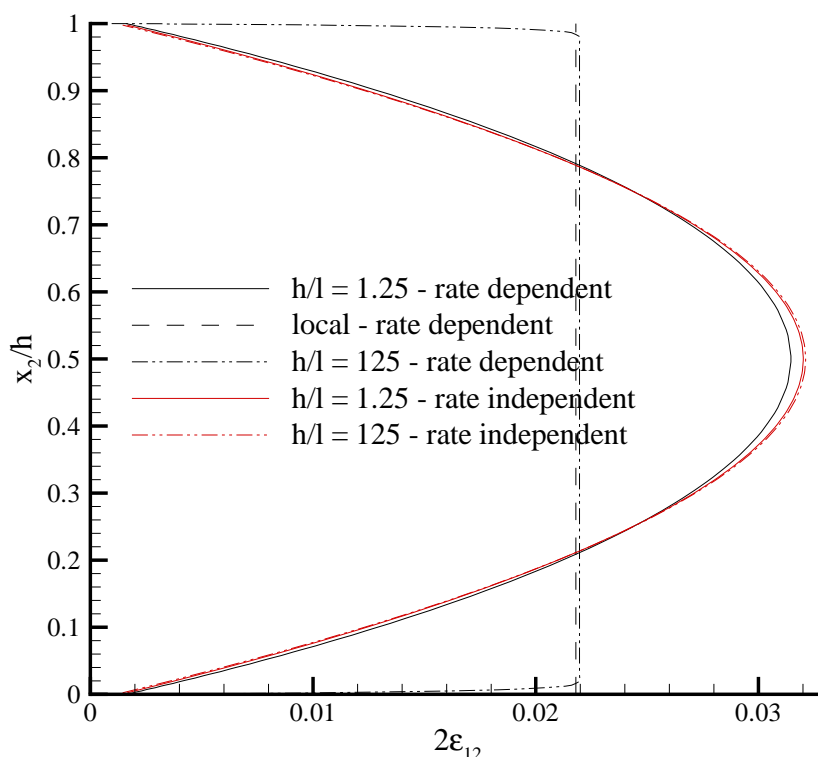


Figure 3: Shear strain distributions with $H = 0$ (no dissipative hardening) comparing the present rate-dependent results with corresponding rate-independent results (Bittencourt et al., 2003) at $\Gamma = 0.0218$.

dislocation calculations, the only boundary conditions are eq. (50) and periodicity. However, for the nonlocal theory microscopic boundary conditions are required. Here we specify micro-free boundary conditions on the sides and micro-clamped boundary conditions on the top and bottom of the region analyzed, i.e.

$$q^{(\beta)} = \xi_i^{(\beta)} n_i = 0 \quad \text{along } x_1 = \pm w \quad (51)$$

$$\gamma^{(\beta)} = 0 \quad \text{along } x_2 = 0, h \quad (52)$$

where $\beta = 1, 2$.

The slip plane orientation is specified by the angle $\theta^{(\beta)} = \pm\theta$, as shown in Figure 1. For the nonlocal theory, field quantities in the solution to this simple shearing boundary value problem are independent of x_1 and macro-equilibrium requires σ_{12} to be spatially uniform and it is the only non-vanishing in-plane stress component.

In order to facilitate comparison with the discrete dislocation results in Bittencourt *et al.* (2003), stress quantities in this Section are normalized by a reference value $\tau_{\text{ref}} = 50$ MPa. Slip systems are oriented at $\theta^{(\beta)} = \pm 60^\circ$. The value of the shear modulus is $\mu = 526\tau_{\text{ref}}$, Poisson's ratio is taken to be $\nu = 0.33$ and the flow strength is specified by $\pi_0 = 0.309\tau_{\text{ref}}$. Various values of the dissipative hardening parameter H are used. The influence of rate-dependent parameters of the constitutive law, (m and \dot{a}) is also studied. When not mentioned their values are $m = 0.04$

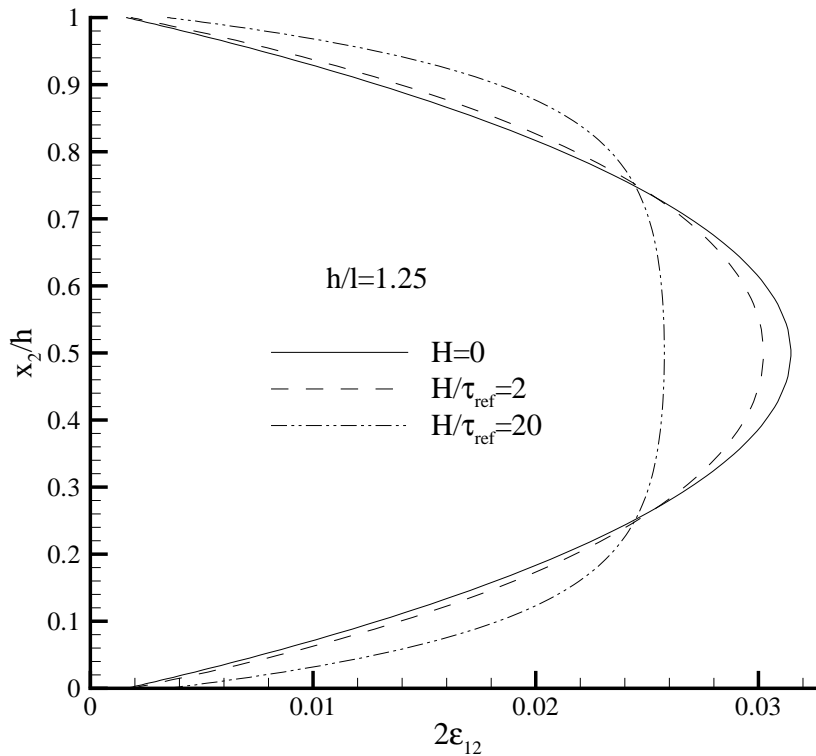


Figure 4: Shear strain distribution with various values of the dissipative hardening H at $\Gamma = 0.0218$.

(which is higher than realistic for a ductile metal crystal at room temperature) and $\dot{a} = 0.001s^{-1}$. Latent hardening was not considered ($q = 0$).

Overall shear stress-shear strain curves for the symmetrically double slipping crystal are shown in Figure 2 for two values of the characteristic length ℓ with no dissipative hardening, i.e. $H = 0$. The rate of shearing $\dot{\Gamma}$ was set equal to the reference rate of shearing $\dot{a} = 0.001s^{-1}$.

Varying h/ℓ by a factor of 100 shows that a small increase of the overall hardening with decreasing size is predicted also by the rate-dependent nonlocal theory. The results here are similar to the rate-independent case in Bittencourt et al. (2003). In Figure 2, in the rate-independent case, a sharp transition occurs from elastic to plastic range, while in the rate-dependent case, the stress-strain curve in this region has a smooth transition which is a rate sensitivity effect, that here is relatively high ($m = 0.04$).

Figure 3 shows the shear strain $2\epsilon_{12} = du_1/dx_2$ distribution for crystals again with $H = 0$. The rate-independent numerical solution (see Figure 3) is coincident with the analytical solution given in Bittencourt et al. (2003), which gives a quadratic plastic slip profile. Numerical solutions for a rate dependent crystal using the present algorithm are also shown in Figure 3. The results are very close to the rate-independent results for a large characteristic length, $h/\ell = 1.25$. However, for $h/\ell = 125$ the shear strain is essentially uniform across most of the layer, with boundary layers at the edges. Thus, in contrast to the rate-independent results for $H = 0$, for a rate dependent crystal a boundary layer profile can develop with $H = 0$.

Three values of the dissipative hardening parameter H were considered: $H/\tau_{ref} = 0.2, 2$ and 20. The effect of non-zero dissipative hardening H at fixed size ($h/\ell = 1.25$) is shown

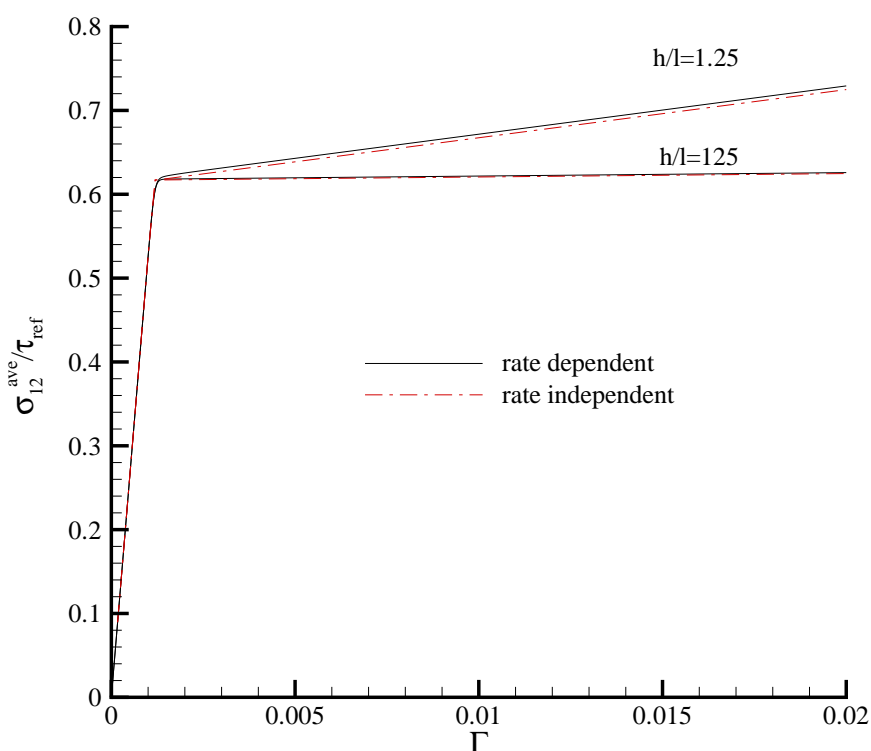


Figure 5: Shear stress-shear strain relations with $H/\tau_{ref} = 0.2$, comparing the present rate-dependent results with corresponding rate-independent results (Bittencourt et al., 2003).

in Figure 4 at $\Gamma = 0.0218$. Dissipative hardening tends to change the shape of shear strain distribution, from parabolic to nearly constant in the crystal bulk with boundary layers at the edges, for H sufficiently large. However, H does not have as strong an effect on the strain distribution as in the rate-independent case, at least for the properties here studied. The tendency to decrease the thickness of the boundary layer with increasing H seen for a rate-independent crystal (Bittencourt et al., 2003) is also observed here. However, a much larger value of H is necessary in the rate-dependent cases to have the same size effect as for the rate independent cases. This tendency apparently depends on the layer size involved, since, the effect of strain hardening on the strain distribution practically vanishes for $h/\ell = 125$. In this case, the strain distribution is nearly uniform over most of the layer regardless the value of H .

Effects of dissipative hardening on the overall shear stress-shear strain curves are shown in figure 5. The results are similar to the rate-independent case, with stresses only slightly higher due to the aforementioned effect of rate sensitivity.

The effect of the rate parameters \dot{a} and m on the overall stress-strain curves and on the strain distribution are shown in Figures 6, 7 and 8. For these calculations, the rate of shearing $\dot{\Gamma}$ was taken equal to $\dot{\Gamma} = 0.1s^{-1}$. In all cases in these figures $h/\ell = 1.25$.

These parameters only change the initial flow stress in the present calculations. No significant change in strain distribution was observed (see Figure 8). For $\dot{a} = 0.1$, the initial flow stress is similar to that for the rate-independent case. In this case the value of \dot{a} is coincident with the overall rate of shearing ($\dot{\Gamma}$) imposed. As seen in Figure 7 the effect of the rates ($\dot{\Gamma}$ or

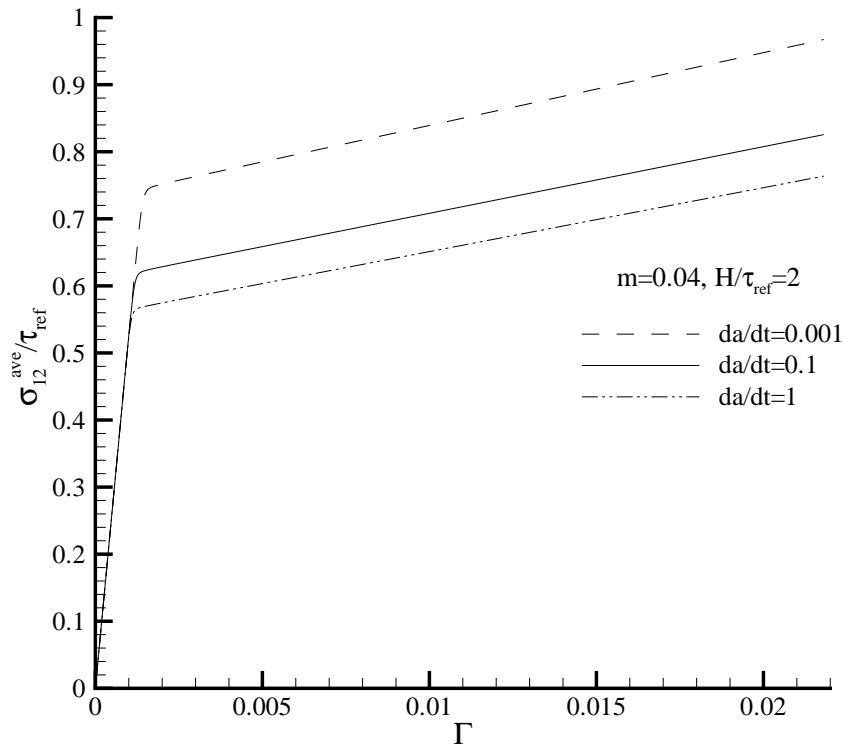


Figure 6: Shear stress-shear strain relations with $H/\tau_{ref} = 2$; ($h/\ell = 1.25$).

\dot{a}), decreases with the value of the rate sensitivity exponent m , as expected.

6 CONCLUDING REMARKS

A finite element implementation of the crystal plasticity theory of Gurtin (2002), considering material rate-dependence has been presented. The implementation was used to solve the problem of a crystal with two symmetric slip systems subject to simple shear. The results show that, as for a rate independent crystal, the theory of Gurtin (2002) is able to capture size effects as seen in the discrete dislocation calculations of Shu et al. (2001). These effects cannot be captured by a local crystal plasticity theory.

The consideration of rate effects does not substantially change the overall stress-strain response when compared to the rate-independent case (since \dot{a} is equal to the prescribed displacement rate $\dot{\Gamma}$, see eq. (6)). The shear distribution throughout the crystal also does not change substantially for large values of the characteristic length ℓ and for low or vanishing dissipative hardening H , i.e., the shear distribution is essentially parabolic regardless the rate effects. However, a much larger dissipative value of hardening is necessary to produce boundary layers for a rate-dependent crystal for large characteristic lengths. But the most notable difference between the two constitutive descriptions occurs when the characteristic length is decreased. In contrast to the rate-independent prediction, boundary layers do appear when dissipative hardening is absent, i.e. when $H = 0$.

The rate-dependent algorithm developed here is equivalent to the conventional forward gra-

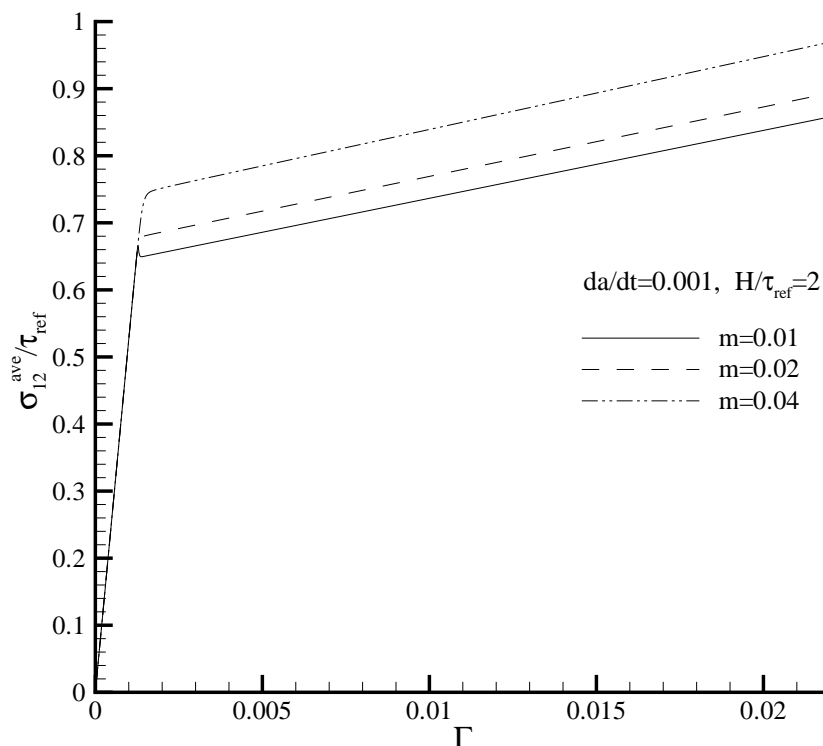


Figure 7: Shear stress-shear strain relations with $H/\tau_{ref} = 2$; ($h/\ell = 1.25$).

cient method when the nonlocal terms are absent. This algorithm has stability advantages when compared to a pure Euler algorithm, since an estimation of the slip values is used in the next time-step, in place of the previous time step values. The algorithm also gains in simplicity when compared to that for rate-independent plasticity, since all Gauss points are visco-plastic and the strong form, eq. (4), of the microscopic balance does not need to be computed. Extensions of the implementation presented here to more than two slip systems and to more complex boundary value problems are being undertaken.

REFERENCES

- Acharya, A. and Bassani, J.L. Incompatibility and crystal plasticity. *J. Mech. Phys. Solids*, 48:1565–1595, 2000.
- Asaro, R.J. and Needleman, A. Texture development and strain hardening in rate dependent polycrystals. *Acta metall.*, 33:923–953, 1985.
- Ashby, M.F. The deformation of plastically non-homogeneous materials. *Phil. Mag.*, 21:399–424, 1970.
- Bittencourt, E., Needleman, A., Gurtin, M.E and Van der Giessen, E. *J. Mech. Phys. Solids*, 51:281–310, 2003.
- Borg, U., Niordson, C.F., Fleck, N.A. and Tvergaard, V. A viscoplastic strain gradient analysis of materials with voids or inclusions. *Int. J. Solids Struct.*, 43:4906–4916, 2006.

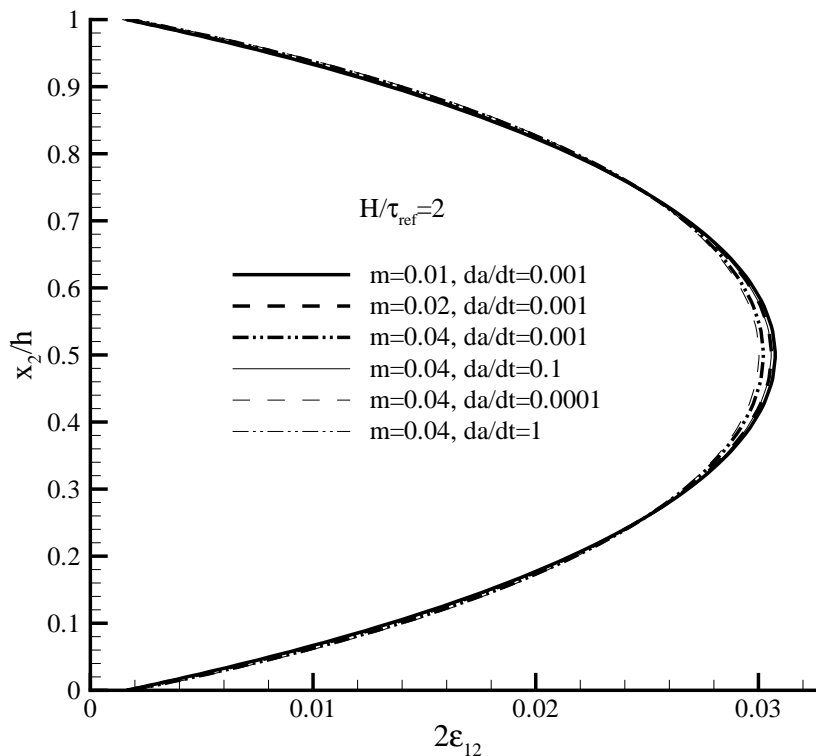


Figure 8: Shear strain distribution with $H/\tau_{ref} = 2$; ($h/\ell = 1.25$).

- Brown, L.M. and Ham, R.K. Dislocation-particle interactions. in: *Strengthening Methods in Crystals* pp. 12–135, Elsevier, Amsterdam, 1971.
- Ebeling, R., Ashby, M. F. Dispersion hardening of copper single crystals. *Phil. Mag.*, 13:805–834, 1966.
- Fleck, N.A. and Hutchinson, J.W. A phenomenological theory for strain gradient effects in plasticity. *J. Mech. Phys. Solids*, 41:1825–1857, 1993.
- Fleck, N.A. and Hutchinson, J.W. Strain gradient plasticity. *Adv. Appl. Mech.*, 33:295–361, 1997.
- Fleck, N.A. and Hutchinson, J.W. A reformulation of strain gradient plasticity. *J. Mech. Phys. Solids*, 49:2245–2271, 2001.
- Fleck, N.A., Muller, G.M., Ashby, F., Hutchinson, J.W. Strain gradient plasticity: theory and experiment. *Acta Metall. Mater.*, 42:475–487, 1994.
- Gurtin, M.E. A gradient theory of single-crystal viscoplasticity that accounts for geometrically necessary dislocations. *J. Mech. Phys. Solids*, 50:5–32, 2002.
- Gurtin, M.E. and Needleman, A. Boundary conditions in small-deformation, single-crystal plasticity that account for Burgers vector. *J. Mech. Phys. Solids*, 53:1–31, 2004.
- Nye, J.F. Some geometrical relations in dislocated solids, *Acta Metall.*, 1:153–162, 1953

- Peirce, D., Asaro, R.J. and Needleman, A. Material rate dependence and localized deformation in crystalline solids. *Acta metall.*, 31:1951–1976, 1983.
- Shu, J. Y., Fleck, N.A., Van der Giessen, E. and Needleman, A. Boundary layers in constrained plastic flow: comparison of nonlocal and discrete dislocation plasticity. *J. Mech. Phys. Solids*, 49:1361–1395, 2001.
- Shu, J.Y. and Fleck, N.A. Strain gradient crystal plasticity: size-dependent deformation of bicrystals. *J. Mech. Phys. Solids*, 47:297–324, 1999.